http://dx.doi.org/10.5012/bkcs.2013.34.1.279

Simple Preparation of Anatase TiO_2 Nanoparticles *via* Pulsed Laser Ablation in Liquid

Seong Min Hong, Seulki Lee, Hyeon Jin Jung, Yiseul Yu, Jae Ho Shin,[†,*] Ki-Young Kwon,[*] and Myong Yong Choi[*]

Department of Chemistry and Research Institute of Natural Science, Gyeongsang National University, Jinju 660-701, Korea
[*]E-mail: kykwon@gnu.ac.kr (K.-Y. Kwon); mychoi@gnu.ac.kr (M. Y. Choi)
[†]Department of Chemistry, Kwangwoon University, Seoul 139-701, Korea. [*]E-mail: jhshin@kw.ac.kr
Received October 8, 2012, Accepted October 10, 2012

Key Words : TiO_2 nanoparticles, Anatase and rutile phase, Pulsed laser ablation in liquid (PLAL), Size distribution

The physical and chemical properties of TiO_2 have been of great interest due to the potential application in photocatalytic, photovoltaic, lithium-ion battery and dye-sensitized solar cell systems.[1-3] Especially, its characteristic properties in optical and electronic properties, nontoxicity, chemical inertness, and high melting temperatures have drawn extensive research on the ability of semiconductor photocatalyst to promote the photodegradation of various pollutants.[4,5] Anatase, brookite, and rutile are the major crystalline structures of TiO_2, of which rutile phase is most stable; whereas anatase and brookite phases are metastable and easily transformed to rutile phase when heated above about 600-800 °C.[6,7] As demonstrated in other experimental studies, the anatase form of TiO_2 has shown much higher photoactivity than that of rutile.[3,5,8,9]

In the meantime, a number of methods have been explored and developed for the synthesis of TiO_2 nanoparticles, such as hydrolysis of Ti(IV) ions,[10] hydrolysis of titanium alkoxides[11] or titanium tetrachloride[12] in gas phase, sol-gel,[13] hydrothermal hydrolysis,[14] and precipitation,[15] of which many studies were devoted to the synthesis of rutile phase, while fewer investigations on the anatase phase. This naively supports that synthesis of pure anatase phase is more challenging than that of rutile. Furthermore, the major products from the above techniques are typically amorphous and require post-calcination for better crystallinity and morphology of the product, which inevitably results in the formation of larger sizes of TiO_2 nanoparticles. Therefore, it is demanding to explore a method that overcomes the problems mentioned above.

In order to fabricate small-sized TiO_2 nanoparticles with good crystallinity at room temperature, we have applied a pulsed laser to ablate a Ti plate immersed in deionized water and methanol. Pulsed laser ablation in liquid (PLAL)[16] was introduced by Patil and co-workers in 1987 and has been demonstrated to be an effective, simple, and versatile method for synthesizing nanomaterials starting from an appropriate choice of solids and liquids.[17-20] Because of relatively simple and clean preparation of nanoparticles using PLAL, coupled with its versatility, many different metal nanostructures providing desired functions have been fabricated. One of the main advantages of PLAL compared to other methods is that it can generate nanomaterials without the need of any catalysts or organic additives. Hence, in recent years, PLAL has become a successful nanomaterial fabrication tool for the formation of the novel nanostructures.[19,21-25] However, compared to large investigations on fabrication of TiO_2 by laser ablation in vacuum,[7,26-31] there were few studies on the preparation of TiO_2 nanoparticles by PLAL.[32-34] Furthermore in the previous PLAL studies, the synthesis of rutile and mixture of anatase and rutile phase was mostly employed.[34,35]

In the present note, we report a one-step synthesis of pure anatase TiO_2 nanoparticles by PLA of Ti plate in deionized (DI) water and methanol in the absence of any surfactants or catalysts at room temperature.

The UV-vis spectrum of as-prepared TiO_2 nanoparticle solution *via* PLA in methanol and DI water is shown in Figure 1 (a, red dotted line) and (b, blue dashed line), respectively. The UV-vis spectrum of commercial TiO_2 sample (Degussa®, P-25, anatase:rutile = 7:3) is also shown to compare the results in Figure 1 (c, black solid line). Exciton absorption band maximum located at about 265 nm is very distinctive for the band gap of anatase TiO_2, which is well-known and extensively reported.[33,35-37] Since TiO_2 is an indirect bandgap semiconductor, the dominant optical absorption arises as the indirect transitions between the valleys.[37,38]

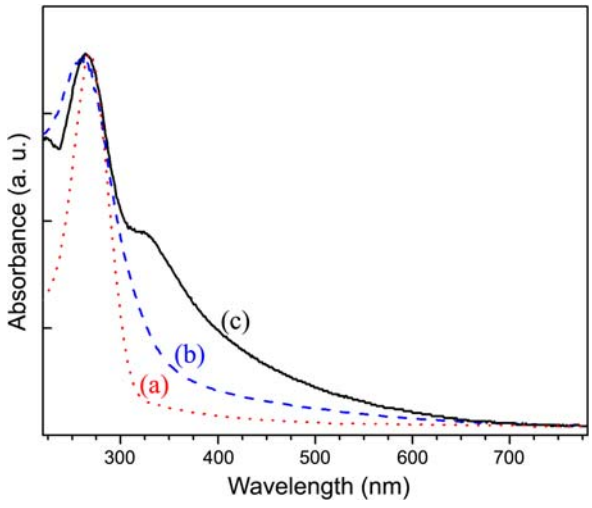

Figure 1. UV-vis absorption spectra of TiO_2 (a) prepared *via* PLA in methanol (red dotted line), (b) in DI water (blue dashed line), and (c) commercial TiO_2 sample (Degussa®, P-25; black solid line).

By extrapolating the absorption band edge as a function of photon energy,[9,39] an indirect bandgap energy (E_g) of anatase phase was obtained to be 3 eV.[33] Since the reference TiO_2 is mixed with anatase and rutile, the absorption spectrum in Figure 1(c) presents a two distinctive band structure, where the higher and lower energy band is attributed to the anatase and rutile phase, respectively. Therefore, we think that the TiO_2 nanoparticles prepared *via* PLAL are anatase phase from the analysis of UV-vis spectrum.

Figure 2 presents the UV-vis absorption spectra of anatase TiO_2 nanoparticles prepared from (a, black solid line) first ablation onto the metal surface in methanol and (b, red dashed line) second ablation to the colloidal solution prepared from the first ablation. The absorption maximum peak for the first and second ablation lies at 269 and 264 nm, respectively. It is shown that the absorption band for the second ablated sample was shifted to the blue of 5 nm. The optical absorption threshold for nanoparticles has known to increase as the size of nanoparticles decreases due to the size quantization effect.[9] Therefore, the mean size of the nanoparticles from the second ablation is expected to be smaller than that of the first ablation.

Figure 3 presents the SEM images of TiO_2 nanoparticles by (a) first and (b) second ablation in methanol to characterize the size and morphology. According to the micrographs, the particles are found to be uniformly distributed and nearly spherical. Furthermore, the size distribution of the particles was statistically analyzed by measuring about 600 nanoparticles. The insets in Figure 3 show the typical size distribution histograms of the nanoparticles prepared at 80 mJ/pulse for 10 min, correspondingly. The histogram fitted with log-normal shows (a) 15.9 ± 0.5 nm and (b) 11.5 ± 0.2 nm, which confirms that the mean size of the nanoparticles decrease after the second ablation to the nanoparticle solution. This size decrease with second laser ablation might be attributed to the further plasma expansion that takes place in thermal adiabatic conditions in all directions at the focused laser beam. This expansion leads to thermal fragmentation of the particles, resulting in the formation of smaller nanoparticles. Thus, the size quantization shifts in the absorption band to higher energy as the particle size decreases in Figure 2 is demonstrated.

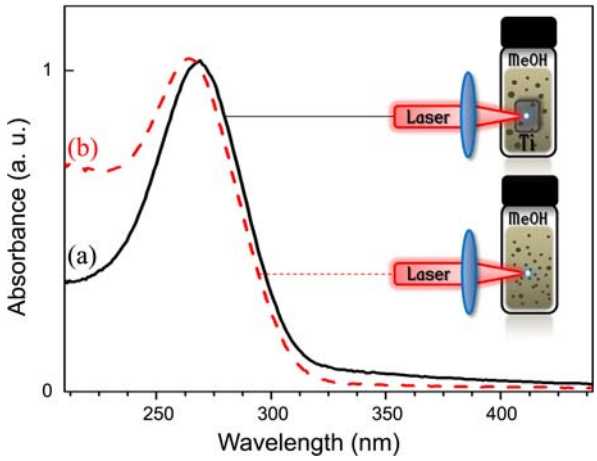

Figure 2. UV-vis absorption spectra of TiO_2 prepared *via* PLA in methanol (a) on the Ti plate (first ablation, black solid line) and (b) to the colloidal solution generated from the first ablation (red dotted line). The corresponding laser ablation experimental schemes (first and second ablation) are shown.

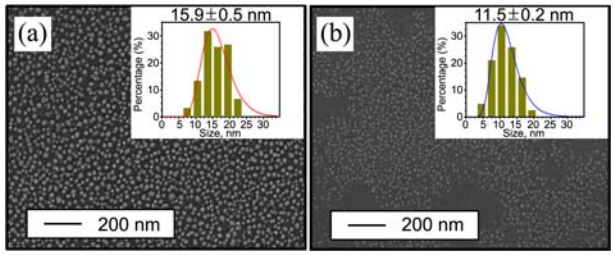

Figure 3. FE-SEM images of TiO_2 prepared *via* PLA in methanol (a) on the Ti plate and (b) to the colloidal solution generated from the first ablation. The corresponding size distribution histograms and mean sizes obtained from the log-normal fit curves (red lines) are shown in the insets.

The SEM and TEM micrographs were employed to exhibit a visual understanding of shape and size distribution of the TiO_2 nanoparticles prepared in DI water as shown in Figure 4. SEM images in Figure 4(a) and (b) taken from a first ablation onto the Ti plate with 80 mJ/pulse for 10 min depict dominant spherically shaped TiO_2 with size distribution of 24.7 ± 0.2 nm, which is relatively larger than that ablated in methanol. According to Figure 4(a), the nanoparticles are uniformly distributed in large area, which is due to an extremely high stability of charged nanoparticles generated from PLAL.[40] Standard and high-resolution TEM micrographs of TiO_2 nanoparticles prepared from the second ablation to the colloidal solutions are presented in Figure 4(c) and (d), respectively. These micrographs reveal that the

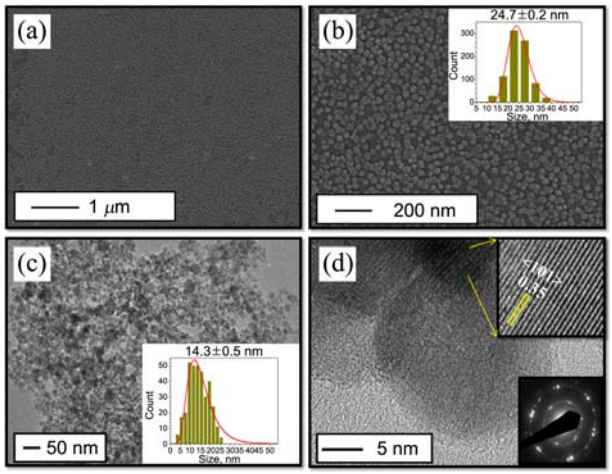

Figure 4. FE-SEM images of TiO_2 prepared *via* PLA on the Ti plate in DI water (a and b). The size distribution histograms and mean sizes obtained from the log-normal fit curves (red lines) are shown in the inset of (b). (c) Standard and (d) high-resolution TEM image of TiO_2 prepared *via* PLA to the colloidal solution generated from the first ablation and the size distribution histograms and mean sizes [inset of (c)] are shown. Top inset of (d): magnified high-resolution TEM image of (d). Bottom inset of (d): SAED pattern.

nanoparticles are also spherical and their crystalline structure with the relative atomic planes. Furthermore, the histogram, shown in the inset of (c), also reveals the mean size of the nanoparticles generated from the second ablation became smaller than that from the first ablation. According to Figures 3 and 4, slightly smaller nanoparticles with a narrow size distribution were obtained in methanol; however, the degrees of size-reduction in the second ablation were larger in DI water. So far, unfortunately there is still no clear explanation of solvent effects with a reduction of nanoparticle sizes.

The corresponding selected-area electron diffraction (SAED) patterns, shown in the insets of Figure 4(d), reveal the well-crystalline structures of TiO_2 nanoparticles. Given that there were many studies of TiO_2 nanoparticles in their amorphous phase but not in their crystalline phase, it is interesting to show the formation of not only well-ordered crystalline structures but also pure anatase phase in this study, which might be attributed to the employed IR wavelength (1064 nm) ablation in liquid. In our preliminary study, we have obtained TiO_2 nanoparticles in their different phases *via* PLAL with shorter wavelength laser ablation, which will be presented in our future study.

To characterize the compositions and structures of the particles, we have obtained the X-ray diffraction (XRD) patterns, shown in Figure 5, of the TiO_2 nanoparticles obtained from the Ti plate ablated in DI water. Figure 5(a) and (b) presents the XRD pattern over a scan interval from 10 to 90° for the as-is sample of TiO_2 *via* PLAL and that of the samples prepared after calcination the as-is sample (a) at 1000 °C, respectively. According to the standard diffraction data over the same scan interval for anatase and rutile, it is seen that the XRD data (a) for the samples obtained *via* PLAL match the standard anatase pattern (JCPDS number: 00-021-1272), while the pattern (b) is matched with the rutile pattern (JCPDS number: 00-021-1276). In order to compare the crystal phase of TiO_2 prepared in this work, we have obtained the XRD pattern of reference TiO_2 sample

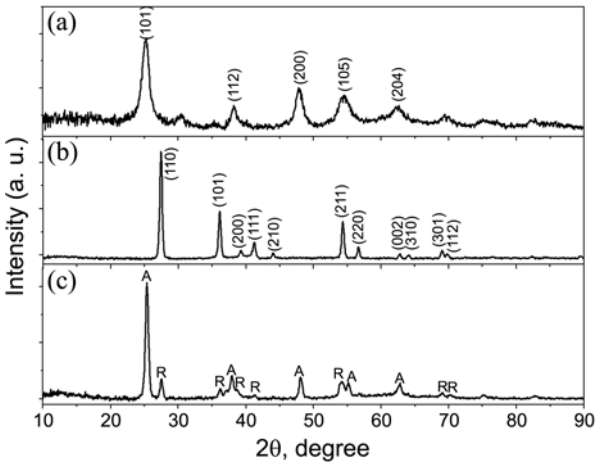

Figure 5. XRD patterns of the TiO_2 (a) prepared *via* PLA on the Ti metal in DI water, (b) after calcination at 1000 °C, and (c) commercial sample (Degussa®, P-25). A: anatase. R: rutile.

(Degussa®, P-25), which contains both anatase and rutile as shown in Figure 5(c). All diffraction peaks in (a) and (b) match with the corresponding TiO_2 peaks in (c).

Since the cooling rate experienced by the metal oxide formed in air can be as fast as 10 K/s,[41] the liquid environment employed in PLA is expected to provide a much faster cooling rate. The formation mechanisms of metal oxides from pure metals in liquid have been proposed and studied in previous studies.[18,19,42,43] Briefly, when single pulsed laser was shot on Ti plate, the high temperature (~6000 K) and high pressure (~1 GPa) provide an ultrasonic adiabatic expansion of the plasma plume, which is cooled quickly by the surrounding solution and hence to interact with solvents.[18] The formation mechanism of TiO_2 nanoparticles can be proposed according to the previously studied mechanisms.[18,19,42,43]

$$Ti_{(clusters)} + H_2O \rightarrow Ti(OH)_4 + H_2 \uparrow$$

$$Ti(OH)_4 \rightarrow TiO_2 + H_2O$$

The extreme local environment in the plasma plume generated in the PLAL process might provide such appropriate conditions for the formation of anatase TiO_2. Unfortunately, the detailed understanding of the formation of anatase TiO_2 nanoparticles is beyond the scope of present study.

In summary, the anatase TiO_2 nanoparticles were successfully synthesized *via* a pulsed Nd-YAG laser (1064 nm) in DI water and methanol at room temperature in the absence of any surfactants or catalysts. TiO_2 nanoparticles fabricated *via* PLAL in this study were nearly spherical and uniformly distributed in large area. Pulsed laser ablation was subsequently applied on the Ti plate and then to the colloidal solution to produce relatively larger and smaller TiO_2 nanoparticles, respectively. As the mean size of the nanoparticles decreases by applying further laser ablation to the nanoparticles generated from the first ablation, the optical absorption threshold becomes increased due to the size quantization effect. The mean size and size distribution of the nanoparticles was investigated from the SEM and TEM images. From the TEM and XRD analysis of the as-is TiO_2 sample, high purity anatase nanoparticles were synthesized, which is also supported by UV-vis absorption spectra. Finally, a formation mechanism of TiO_2 *via* PLAL is proposed. This unique method for the production of pure anatase TiO_2 nanoparticles is a promising tool for the generation of small sized materials, especially metastable and high-temperature phase materials at room temperature, which is cumbersome in other conventional methods. Furthermore, employing this method for generating of small sized-anatase TiO_2 nanoparticles can promote for the study of further applications, such as phtocatalytic, photovoltaic, and dye-sensitized solar cell systems.

Experimental Section

A solid Ti (99.999%, Sigma-Aldrich) plate was ablated by pulsed nanosecond laser in pure water and methanol. The experimental setup is described in detail elsewhere.[17,44,45]

Briefly, the Ti plate was fixed in a Pyrex *via*l filled with 3° DI water (10 mL) continuously stirred by a magnetic bar. A pulsed Nd:YAG laser (1064 nm, 10 Hz, 7 ns) was focused onto the surface of the Ti plate with a spot size of about 1 mm in diameter using a lens with a focal length of 25 mm. The laser ablation was continued for 10 min with laser pulse energy of 80 mJ/pulse. A second laser ablation was applied to the prepared colloidal solution with the same experimental condition as the first ablation step. The ablated solutions were collected at a centrifugation rate of 13000 rpm for 10 min; the resulting sediments were collected and then sonicated after addition of the corresponding solvent and centrifuged a number of times. The experiment was performed for at least 10 times and the products or sediments were collected and dried on a silicon substrate at room temperature. The morphology and structure of the nanoparticles produced by PLAL were investigated with a field emission scanning electron microscope [FE-SEM, XL30 S FEG, Philips (15 kV)] and transmission electron microscope [TEM, JEOL, JEM-2-10 (200 kV)]. X-ray diffraction (XRD) patterns of the nanoparticles were obtained with a Bruker AXS D8 DISCOVER with GADDS diffractometer using Cu Kα (0.1542 nm) radiation with Bragg angle ranging from 10 to 90°.

Acknowledgments. This work was supported by the National Research Foundation (KRF) grant funded by the Korea government (MEST) (2010-0005493) and Korea Ministry of Environment as "GAIA Project" (2012000550026). J. H. Shin also acknowledges the support from the NRF funded by MEST (No. 2010-0005532) and a grant from Kwangwoon University.

References

1. Lundqvist, M. J.; Nilsing, M.; Persson, P.; Lunell, S. *Int. J. Quantum. Chem.* **2006**, *106*, 3214.
2. Subramanian, V.; Karki, A.; Gnanasekar, K. I.; Eddy, F. P.; Rambabu, B. *J. Power Sources* **2006**, *159*, 186.
3. Li, G.; Li, L.; Boerio-Goates, J.; Woodfield, B. F. *J. Am. Chem. Soc.* **2005**, *127*, 8659.
4. Chen, J.; Eberlein, L.; Langford, C. H. *J. Photochem. Photobiol., A* **2002**, *148*, 183.
5. Sivalingam, G.; Nagaveni, K.; Hegde, M. S.; Madras, G. *Appl. Catal., B* **2003**, *45*, 23.
6. Czanderna, A. W.; Ramachandra Rao, C. N.; Honig, J. M. *Trans. Faraday Soc.* **1958**, *54*, 1069.
7. Nakamura, T.; Ichitsubo, T.; Matsubara, E.; Muramatsu, A.; Sato, N.; Takahashi, H. *Acta Mater.* **2005**, *53*, 323.
8. Fujishima, A.; Honda, K. *Nature* **1972**, *238*, 37.
9. Madhusudan Reddy, K.; Gopal Reddy, C. V.; Manorama, S. V. *J. Solid State Chem.* **2001**, *158*, 180.
10. Matijeviæ, E.; Budnik, M.; Meites, L. *J. Colloid Interface Sci.* **1977**, *61*, 302.
11. Kominami, H.; Takada, Y.; Yamagiwa, H.; Kera, Y.; Inoue, M.; Inui, T. *J. Mater. Sci. Lett.* **1996**, *15*, 197.
12. Shi, L.; Li, C.; Chen, A.; Zhu, Y.; Fang, D. *Mater. Chem. Phys.* **2000**, *66*, 51.
13. Sakai, H.; Kawahara, H.; Shimazaki, M.; Abe, M. *Langmuir* **1998**, *14*, 2208.
14. Wu, M.; Long, J.; Huang, A.; Luo, Y.; Feng, S.; Xu, R. *Langmuir* **1999**, *15*, 8822.
15. Chen, J.; Gao, L.; Huang, J.; Yan, D. *J. Mater. Sci.* **1996**, *31*, 3497.
16. Patil, P. P.; Phase, D. M.; Kulkarni, S. A.; Ghaisas, S. V.; Kulkarni, S. K.; Kanetkar, S. M.; Ogale, S. B.; Bhide, V. G. *Phys. Rev. Lett.* **1987**, *58*, 238.
17. Mafuné, F.; Kohno, J.-y.; Takeda, Y.; Kondow, T.; Sawabe, H. *J. Phys. Chem. B* **2000**, *104*, 9111.
18. Zeng, H.; Cai, W.; Li, Y.; Hu, J.; Liu, P. *J. Phys. Chem. B* **2005**, *109*, 18260.
19. Niu, K. Y.; Yang, J.; Kulinich, S. A.; Sun, J.; Li, H.; Du, X. W. *J. Am. Chem. Soc.* **2010**, *132*, 9814.
20. Yang, G. W. *Prog. Mater Sci.* **2007**, *52*, 648.
21. Yan, Z.; Bao, R.; Huang, Y.; Chrisey, D. B. *J. Phys. Chem. C* **2010**, *114*, 11370.
22. Zhang, X.; Zeng, H.; Cai, W. *Mater. Lett.* **2009**, *63*, 191.
23. Pan, C.; Chen, S.-Y.; Shen, P. *J. Phys. Chem. B* **2006**, *110*, 24340.
24. Mafuné, F.; Kohno, J.-Y.; Takeda, Y.; Kondow, T. *J. Phys. Chem. B* **2002**, *106*, 7575.
25. Park, D. K.; Lee, S. J.; Lee, J. H.; Choi, M. Y.; Han, S. W. *Chem. Phys. Lett.* **2010**, *484*, 254.
26. Zheng, H. Y.; Qian, H. X.; Zhou, W. *Appl. Surf. Sci.* **2008**, *254*, 2174.
27. Yamamoto, S.; Sumita, T.; Sugiharuto; Miyashita, A.; Naramoto, H. *Thin Solid Films* **2001**, *401*, 88.
28. Tsai, M. H.; Chen, S. Y.; Shen, P. *J. Aerosol. Sci.* **2005**, *36*, 13.
29. Syarif, D. G.; Miyashita, A.; Yamaki, T.; Sumita, T.; Choi, Y.; Itoh, H. *Appl. Surf. Sci.* **2002**, *193*, 287.
30. Sasaki, T.; Beck, K. M.; Koshizakai, N. *Appl. Surf. Sci.* **2002**, *197-198*, 619.
31. Sanz, M.; Walczak, M.; Oujja, M.; Cuesta, A.; Castillejo, M. *Thin Solid Films* **2009**, *517*, 6546.
32. Tian, F.; Sun, J.; Yang, J.; Wu, P.; Wang, H. L.; Du, X. W. *Mater. Lett.* **2009**, *63*, 2384.
33. Jafarkhani, P.; Dadras, S.; Torkamany, M. J.; Sabbaghzadeh, J. *Appl. Surf. Sci.* **2010**, *256*, 3817.
34. Singh, S. C.; Swarnkar, R. K.; Gopal, R. *J. Nanosci. Nanotechno.* **2009**, *9*, 5367.
35. Barreca, F.; Acacia, N.; Barletta, E.; Spadaro, D.; Currò, G.; Neri, F. *Appl. Surf. Sci.* **2010**, *256*, 6408.
36. Sugimoto, T.; Zhou, X.; Muramatsu, A. *J. Colloid Interface Sci.* **2003**, *259*, 43.
37. Iwabuchi, A.; Choo, C.-K.; Tanaka, K. *J. Phys. Chem. B* **2004**, *108*, 10863.
38. Emeline, A. V.; Ryabchuk, V. K.; Serpone, N. *J. Phys. Chem. B* **2005**, *109*, 18515.
39. Madhusudan Reddy, K.; Manorama, S. V.; Ramachandra Reddy, A. *Mater. Chem. Phys.* **2003**, *78*, 239.
40. Mortazavi, S. Z.; Parvin, P.; Reyhani, A.; Golikand, A. N.; Mirershadi, S. *J. Phys. Chem. C* **2011**, *115*, 5049.
41. Levi, C. G.; Jayaram, V.; Valencia, J. J.; Mehrabian, R. *J. Mater. Res.* **1988**, *3*, 969.
42. Lee, Y.-P.; Liu, Y.-H.; Yeh, C.-S. *Phys. Chem. Chem. Phys.* **1999**, *1*, 4681.
43. Lee, S.; Ahn, A.; Choi, M. Y. *Phys. Chem. Chem. Phys.* **2012**, *14*, 15677.
44. Zeng, H.; Li, Z.; Cai, W.; Cao, B.; Liu, P.; Yang, S. *J. Phys. Chem. B* **2007**, *111*, 14311.
45. Sasaki, T.; Shimizu, Y.; Koshizaki, N. *J. Photochem. Photobiol., A* **2006**, *182*, 335.